Spectroscopic Imaging of Prostate Cancer: A Novel Spectrum Processing Approach and Comparison with the Step-Section Histology

J. Weis[1], H. Ahlström[1], P. Hlavcak[2], M. Häggman[3], F. Ortiz-Nieto[1], and A. Bergman[1]

[1]Department of Radiology, Uppsala University Hospital, Uppsala, Sweden, [2]Department of Pathology, Uppsala University Hospital, Uppsala, Sweden, [3]Department of Urology, Uppsala University Hospital, Uppsala, Sweden

Introduction: Magnetic resonance spectroscopic imaging (MRSI) of the prostate is a challenge. Water and fat suppression is often inadequate, resulting in baseline distortions and water/lipid contamination that prevent accurate estimates of spectral intensities. Two weaknesses of many previous spectroscopic studies can be pointed out. The first is user dependent spectrum processing, especially baseline correction and unclear prior knowledge used in the spectral lines fitting. Verification of MRSI findings can be considered as the second weakness. The majority of previous reports have used sextant biopsy results to evaluate the accuracy of MRSI. Biopsy is, however, subject to sampling errors due to the finite number of cores that can be obtained. It has been reported that up to 30% of cancers were missed at sextant biopsy. Only a few research groups used prostatectomy step section histology systematically as the gold standard of reference (1, 2). This work addresses the novel spectrum evaluation approach based on the combination of vendor optimized spectrum preprocessing in the MR scanner and user independent time-domain spectrum processing in magnetic resonance user interface (MRUI) (3). User independency was achieved by definition of all pre-processing steps and prior knowledge of the fitting algorithm. Our objective was quantitation of (Cho+Cr)/Cit ratio in normal and pathologic human prostate and comparison of the results with histopathology after radical prostatectomy.

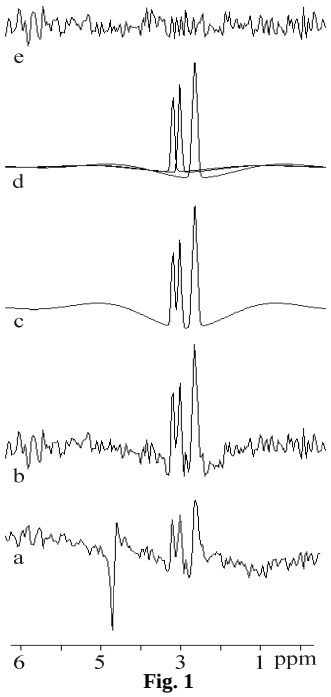

Fig. 1

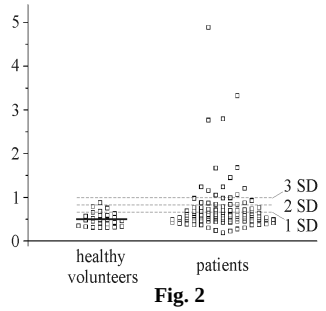

Fig. 2

Materials and Methods: Four healthy volunteers (mean age of 55.8±13.6 years, range 39-71 years) and thirteen patients with biopsy-proven prostate cancer (mean age, 61.2±4.4 years, range 54-66 years) were measured. None of the patients had undergone any therapy before MR examination and surgery. Radical prostatectomy was performed within one week after MRSI. Following surgery, radical prostatectomy specimens were serially sectioned at 4 mm intervals, embedded in paraffin and Gleason score was evaluated. All data were acquired on a 1.5 T Gyroscan Intera scanner (Philips) with an endorectal coil. 2D MRSI was performed using PRESS technique (TR/TE 1200/130 ms, matrix 16x16, FOV 150 mm, circular phase encoding with reduction factor of 25%, slice thickness 20 mm, spectral bandwidth 1000 Hz, 512 spectral data points, 3 acquisitions). Net measurement time was 12.5 minutes. We used relatively large nominal voxel sizes (0.9x0.9x2 cm^3) to be able to cover the most part of the prostate within one 2D MRSI measurement. Water signal was suppressed using BASING (4) and lipids were suppressed by a frequency-selective inversion recovery pre-pulse. A rapid MRSI of the water signal was performed prior to the actual measurement. The initial vendor optimized data processing steps were performed in the MR scanner. Data were filtered in the both phase-encoding dimensions with a Hanning filter and zero filled. Time-domain signals were apodized with a Lorentz-Gauss function (5,-1,-3) Hz. A digital shift accumulation (DSA) filter was applied to suppress residual water signal and to enhance Cit spectral region. The spectra were then corrected for the frequency shifts caused by B_0 deviations utilizing the non-water suppressed data set. The resulting spectra were transferred to a PC and inverse Fourier transformed to the time domain and zero filled to 1024 complex points (Fig. 1a). Spectrum processing continued in the time domain using MRUI. Residual water and lipid resonances were removed by applying a HLSVD filter. Baseline correction was performed by truncation of the first two points of the FID (Fig. 1b). Cho, Cr and Cit spectral lines were fitted by Gaussians and AMARES algorithm (5) (Fig. 1c,d). The following prior knowledge was imposed. The positions of the Cho and Cit peaks were estimated by AMARES with the soft constrain 2.6±0.1 and 3.2±0.1 ppm. Position of Cr was determined using fixed shift -0.171 ppm in respect of Cho. Linewidth of Cit was estimated by AMARES. Linewidths of the Cho and Cr were determined by multiplication of the Cit linewidth by fixed values 0.897 and 0.776, respectively. The linewidth ratios between Cit, Cho, and Cr were obtained by fitting a series of well resolved spectra of the healthy volunteers. For the cancer spectra with the highest Cho spectral line and less resolved Cit, the position of Cit peak was determined using fixed shift -0.562 ppm in respect of Cho. Linewidth of Cho was estimated by AMARES. Linewidths of the Cr and Cit were computed by multiplication of the Cho linewidth by fixed values 0.892 and 1.17, respectively. Standard deviation (SD) of the FID amplitude of a certain spectral component was used as a measure for estimation accuracy and noise level. Only spectra with Cho and Cit amplitudes five times greater than their SDs were used in quantitation. This condition reliably excluded noisy spectra and/or spectra having artifacts that obscured evaluation. Each voxel was classified as healthy, ambiguous, suspicious and very suspicious for cancer (6). Voxel were considered ambiguous for cancer if the ratio of (Cho+Cr)/Cit was more than 1, but 2 or fewer SDs above the mean normal value. Voxels were assigned suspicious for cancer with a (Cho+Cr)/Cit ratio more than 2, but 3 or fewer SDs above the healthy ratio. Voxels were considered to be very suspicious for cancer if (Cho + Cr)/Cit ratio was more than 3 SDs above the average normal value.

Results: Figure 1 illustrates the proposed spectrum processing approach. Preprocessed spectrum exported from the scanner is shown in Fig. 1a. Figure 1b-e demonstrates MRUI processing: HLSVD water/fat filtering and baseline correction (b), fitting results (c, d), and residue (e). Scatterplots of the (Cho+Cr)/Cit ratios of all evaluated voxels of normal volunteers and patients are shown in Fig. 2. Mean value 0.50±0.16 of healthy volunteers is depicted by a horizontal thick line. The dashed lines represent one, two, and three SDs from the mean value of the normal volunteers. Two patients with Gleason score (3+3) and (4+5) had normal (Cho+Cr)/Cit ratio in all measured voxels. These patients were evaluated as false negative for cancer. Three patients with the Gleason score (3+3), (3+4), and (4+3), were classified to ambiguous category by at least one voxel. The (Cho+Cr)/Cit ratio of the remaining eight patients reached both suspicious and very suspicious levels. Gleason scores of these patients were between (3+3) and (5+4).

Discussion and Conclusions: This study has confirmed that 2D proton MRSI is able to detect differences in the relative levels of prostate metabolites Cit, Cho, and Cr between prostate cancer and normal tissue in the peripheral and transition zone. Original feature of the proposed data processing approach is combination of the vendor optimized frequency domain spectrum preprocessing in MR scanner and user independent time domain processing in MRUI software package. User independency was achieved by defining the spectrum pre-processing and prior knowledge. MRUI processing minimized subjective data manipulation and interpretation. In agreement with the previous studies (2, 6, 7) our results show considerable overlap of metabolite ratios between cancer and normal prostate tissue at various Gleason score levels (Fig. 2). We did not find trend or correlation between the (Cho+Cr)/Cit ratio and Gleason score. This finding is in disagreement with the previous study (2). Note that our patient group was too small for reliable evaluation of such a relation.

References: (1) Wefer AE et al, J Urol 2000;164:400-404. (2) Zakian KL et al, Radiology 2005;234:804-814. (3) Naressi A et al, MAGMA 2001;12:141-152. (4) Star Lack J et al, Magn Reson Med 1997;38:311-321. (5) Vanhamme L et al, J Magn Reson 1997;129:35-43. (6) Kurhanewitz J et al, Radiology 1996;198:795-805. (7) Kelm MB et al, Magn Reson Med 2007;57:150-159.

Acknowledgement: Supported by the Swedish Research Council (K2006-71X-06676-24-3).